CERN-TH/99-209
nucl-th/9907060

Primordial hadrosynthesis in the Little Bang

Ulrich Heinz[a*]

[a]Theoretical Physics Division, CERN, CH-1211 Geneva 23

The present status of soft hadron production in high energy heavy-ion collisions is summarized. In spite of strong evidence for extensive dynamical evolution and collective expansion of the fireball before freeze-out I argue that its chemical composition is hardly changed by hadronic final state interactions. The measured hadron yields thus reflect the primordial conditions at hadronization. The observed production pattern is consistent with statistical hadronization at the Hagedorn temperature from a state of uncorrelated, color deconfined quarks and antiquarks, but requires non-trivial chemical evolution of the fireball in a prehadronic (presumably QGP) stage *before* hadron formation.

1. Heavy-ion data and the nuclear phase diagram

Relativistic heavy-ion collisions are studied with the goal of creating hot and dense hadronic matter and to investigate the nuclear phase diagram at high temperatures and densities, including the expected phase transition to a color deconfined quark-gluon plasma. But even if the energy deposited in the reaction zone is quickly randomized and the fireball constituents reach an approximate state of local thermal equilibrium, a simple connection between heavy-ion observables and the phase diagram is still not easy: the pressure generated by the thermalization process blows the fireball apart, causing a strong time dependence of its thermodynamic conditions which is difficult to unfold from the experimental observations. There are therefore two fundamental issues to be solved before one can extract information on the nuclear phase diagram from heavy-ion experiments: (1) To what degree does the fireball approach local thermal equilibrium? (2) Which observables are sensitive to which stage(s) of its dynamical evolution, and which is the most reliable procedure for extracting the corresponding thermodynamic information?

Combining microscopic models for the dynamical fireball evolution with macroscopic thermal models for the analysis of heavy-ion data, significant progress has been recently made in answering both of these questions. Crucial for this achievement was the dramatically improved quantity and quality of hadron production data from the analysis of collisions between very heavy nuclei (Au+Au, Pb+Pb) from SIS to SPS.

Fig. 1 shows a compilation by Cleymans and Redlich [1] of hadronic freeze-out points in the nuclear phase diagram from various collision systems and beam energies. The upper set of points, parametrized by a constant average energy per particle $\langle E\rangle/\langle N\rangle$=1 GeV [1], is obtained from measured hadron yields. They indicate the average thermodynamic conditions at *chemical freeze-out* when the hadron abundances stopped evolving. The lower

*On leave from Institut für Theoretische Physik, Regensburg; work supported by BMBF, DFG, and GSI.

set of points, compared with lines of constant energy and particle density [1], is obtained from analyses of hadron momentum spectra and/or two-particle momentum correlations. They indicate *thermal freeze-out*, i.e. the decoupling of the momentum distributions. The chemical and thermal freeze-out points at the SPS and AGS, respectively, are connected by isentropic expansion trajectories with $S/B \approx$ 36-38 for the SPS and 12-14 for the AGS.

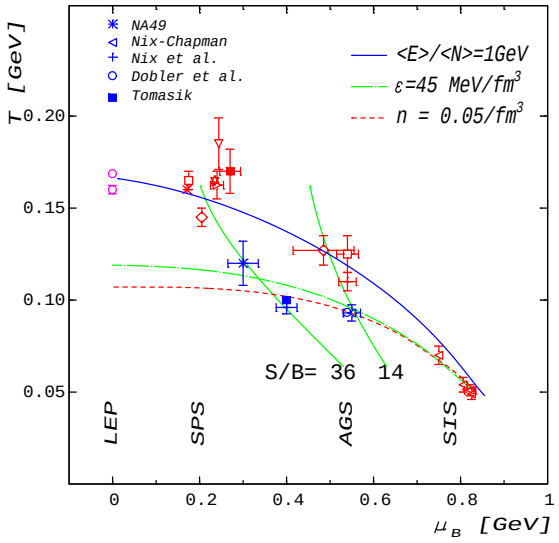

Figure 1. Compilation by Cleymans and Redlich [1] of chemical and thermal freeze-out points. The legend refers to the symbols for the thermal freeze-out points. For the original references for all the data points see [1].

My first goal is a critical discussion of how these freeze-out parameters were extracted from the data and how reliable Fig. 1 is. Following that is a more detailed study of the fireball properties at chemical freeze-out, taking into account additional information not contained in Fig. 1, and a discussion of a consistent dynamical picture which can explain Fig. 1. My main conclusion, based on a chain of arguments developed and sharpened over the last few years [2], is given in the abstract; similar conclusions were reached and recently publicized by R. Stock [3] and are also found in E. Shuryak's talk [4].

2. Thermal freeze-out, "Hubble"-flow, and the Little Bang

Let me begin with a discussion of the thermal freeze-out points. Freeze-out marks the transition from a strongly coupled system, which evolves from one state of local thermal equilibrium to another, to a weakly coupled one of essentially free-streaming particles. If this transition happens quickly enough, the thermal momentum distributions (superimposed by collective expansion flow) are frozen in, and the temperature and collective flow velocity at the transition "point" can be extracted from the measured momentum spectra. In high energy heavy-ion collisions the freeze-out process is triggered dynamically by the accelerating transverse expansion and the very rapid growth of the mean free paths as a result of the fast dilution of the matter [5]. Idealizing the kinetic freeze-out process by a single point in the phase diagram is therefore not an entirely unreasonable procedure.

As in the Big Bang, the observed momentum spectra mix the thermal information with the collective dynamics of the system. In the Big Bang, the observed microwave background radiation has a Bose-Einstein energy spectrum with an "effective temperature" (inverse slope) which is *redshifted* by cosmological expansion down from the original freeze-out temperature of about 3000 K to an observed value of only 2.7 K. In the Little Bang, where we observe the *thermal hadron radiation* from the outside, the transverse mo-

mentum spectra are *blueshifted* by the collective transverse motion towards the observer. Simple approximate expressions which capture this effect are[1] $T_{\rm slope} \approx T_{\rm therm} + \frac{1}{2} m \langle v_\perp \rangle^2$ (which applies for $p_\perp \ll m$) and $T_{\rm slope} \approx T_{\rm therm} \sqrt{(1+\langle v_\perp \rangle)/(1-\langle v_\perp \rangle)}$ (which is good for $p_\perp \gg m$). For a given species (fixed m) the measured slope of the spectrum is thus ambiguous: temperature and flow cannot be separated.

The ambiguity can be lifted in two ways: (i) One performs a simultaneous fit of the $m_\perp$-spectra of hadrons with different rest masses, thereby exploiting the mass dependence in the first of these two expressions [7]. This makes the implicit assumption that thermal freeze-out happens simultaneously for all particle species. For Au+Au collisions at the AGS this works well and gives $T_{\rm therm} \approx 93$ MeV and $\langle v_\perp \rangle \approx 0.5\,c$ at midrapidity [8]. Or (ii) one concentrates on a single particle species and correlates (as described in detail by U. Wiedemann [9]) their spectra with their two-particle Bose-Einstein correlations. The $M_\perp$-dependence of the transverse HBT radius parameter[2] $R_\perp(M_\perp) \approx R/\sqrt{1 + \xi \langle v_\perp \rangle^2 \frac{M_\perp}{T_{\rm therm}}}$ then provides an orthogonal correlation between temperature and flow, allowing for their separation. For pions from Pb+Pb collisions at the SPS this leads again to kinetic freeze-out temperatures of 90–100 MeV and average tranverse flow velocities of 0.5–0.55 c (perhaps even somewhat higher at midrapidity) [9,10].

This fixes the position of the freeze-out point along the T-axis in Fig. 1, but what about $\mu_{\rm B}$? Since chemical equilibrium is already broken earlier, at $T_{\rm chem} \approx 170 - 180$ MeV (see below), $\mu_{\rm B}$ is, strictly speaking, not well-defined. In order to still be able to associate with kinetic freeze-out a point in the phase-diagram one commonly adjusts $\mu_{\rm B}$ in such a way that the deviations between the observed particle ratios and their chemical equilibrium values at $T_{\rm therm}$ are minimized. This is acceptable if the deviations are small; in practice they can approach a factor 2 or so. This clearly causes irreducible systematic uncertainties in the baryon chemical potential at thermal freeze-out which are usually not evaluated and are not included in the horizontal error bars in Fig. 1 (where given).

Let's nonetheless accept these thermal freeze-out parameters and now ask the question: *How did the system get there?* Does the implied picture of a rapidly expanding, locally thermalized fireball, *the Little Bang*, make sense? These questions can be studied by microscopic kinetic simulations of RQMD, URQMD and HSD [11] type; even if they do not include quark-gluon degrees of freedom during the very dense initial stages and thus may parametrize the initial hadron production incorrectly (see below), they can be used to explore the effects of scattering among the hadrons before kinetic freeze-out and the evolution of collective flow. A detailed study of thermalization by rescattering was recently performed by the URQMD group for Au+Au and Pb+Pb collisions from AGS to SPS energies [12] (Fig. 2). After an initial non-equilibrium stage lasting for about 8–10 fm/c these systems reach a state of approximate local thermal equilibrium which expands and cools at roughly constant entropy for another 10 fm/c before decoupling. During the adiabatic expansion stage strong collective flow builds up. Thermalization is driven by

[1] This is accurate for non-relativistic particles from a Gaussian source with a linear transverse velocity profile $v_\perp(r) = \langle v_\perp \rangle \frac{r}{r_{\rm rms}}$, where $\langle v_\perp \rangle$ is the radial velocity at the rms radius $r^2_{\rm rms} = \langle x^2 + y^2 \rangle$. The analogous formula in [6] lacks the factor $\frac{1}{2}$ in the second term since it uses the radial velocity at $r = r_{\rm rms}/\sqrt{2}$.

[2] $\xi \sim \mathcal{O}(1)$ accounts for different transverse density and flow profiles; $\xi = \frac{1}{2}$ for the case described in fn. 1.

intense elastic rescattering, dominated by resonances (e.g. $\pi+N\rightarrow\Delta\rightarrow\pi+N$); inelastic processes are much rarer and lead only to minor changes in the chemical composition of the fireball [13,14]. As a result, significant deviations from chemical equilibrium occur which increase with time; most importantly, at thermal freeze-out one sees a large pion excess which can only partially be accounted for by the initial string fragmentation process [12]. Remarkably, these deviations from chemical equilibrium produce very little entropy [12]. The S/B values extracted from the URQMD simulations agree with those from the thermal model analysis of the data (cf. Figs. 1 and 2).

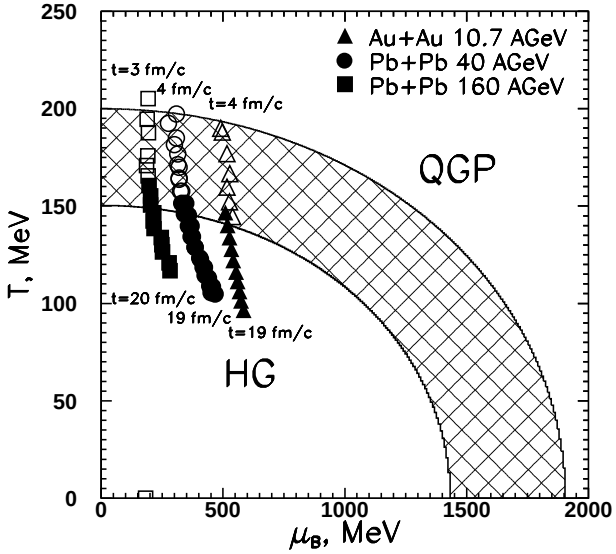

Figure 2. Expansion trajectories from URQMD simulations [12]. Open and closed symbols denote the pre-equilibrium and hydrodynamic stages, respectively, of the collision in steps of 1 fm/c. The filled symbols lie on lines of constant entropy per baryon, S/B=38, 20, 12 for 160, 40, 10.7 A GeV, respectively [12]. The shaded region indicates the expected parameter range for the deconfining phase transition.

Hadron momentum spectra and two-particle correlations thus provide strong evidence for the existence of the Little Bang: thermal hadron radiation with $T_{\rm therm} \approx 90-100$ MeV and strong 3-dimensional ("Hubble-like") expansion with transverse flow velocities $\langle v_\perp \rangle \approx 0.5-0.55\,c$ (and even larger longitudinal ones [5,8]). These two observations play a similar role here as the discovery of Hubble expansion and the cosmic microwave radiation played for the Big Bang. But is there also a heavy-ion analogy to primordial Big Bang nucleosynthesis? In the following section I will argue that we have indeed evidence for "primordial hadrosynthesis" in the Little Bang.

3. Thermal models for chemical freeze-out and "primordial hadrosynthesis"

Chemical reactions, which exploit small inelastic fractions of the total cross section, are typically much slower than the (resonance dominated) elastic processes. One thus expects chemical freeze-out to occur *before* thermal freeze-out [15] ($T_{\rm chem} > T_{\rm therm}$) but on an expansion trajectory with roughly the same entropy per baryon S/B. Fig. 1 suggests that this is indeed the case. This is analogous to the Big Bang where nucleosynthesis happened after about 3 minutes at $T_{\rm chem} \approx 100$ keV whereas the microwave background decoupled much later, after about 300000 years at $T_{\rm therm} \approx \frac{1}{4}$ eV. The much smaller difference between the two decoupling temperatures in the Little Bang is mainly due to its much (about 18 orders of magnitude) faster expansion rate.

Before discussing implications of the chemical freeze-out points in Fig. 1 I first explain how they were obtained. Can thermal models be used to analyze chemical freeze-out?

I discussed this question in some detail last year in Padova [2] and thus will be short here. The first difficulty arises from the collective expansion which strongly affects the shape of the $m_\perp$- and y-spectra, in a way which depends on the particle mass. However, many experiments measure the particle yields only in small windows of $m_\perp$ and y. A chemical analysis of particle ratios from such experiments depends very strongly on model assumptions about the fireball dynamics [16]. Static fireball fits yield chemical freeze-out parameters which are quite sensitive to the rapidity window covered by the data [17]. Flow effects drop out, however, from 4π-integrated particle ratios as long as freeze-out occurs at constant T and μ. 4π yields thus minimize the sensitivity to the collective fireball dynamics and are preferable for thermal model analyses.

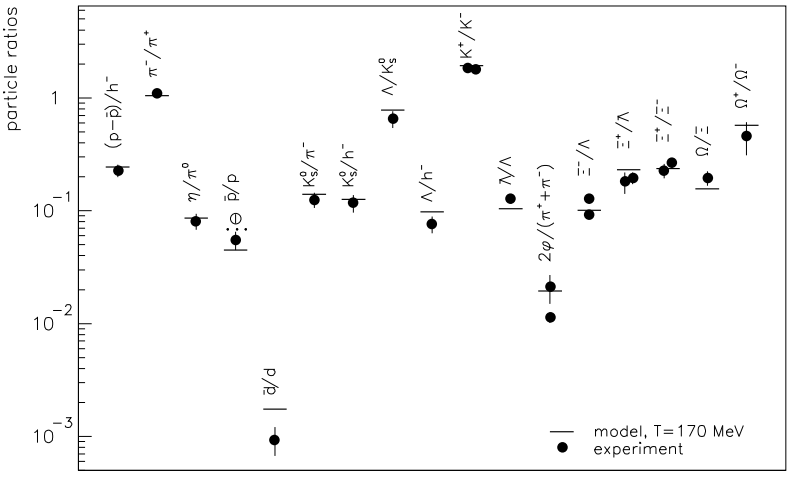

Figure 3. Comparison between thermal model predictions and data for 158 A GeV Pb+Pb collisions, after optimizing the model parameters $T_{\rm chem}$=170 MeV, $\mu_{\rm B}$=270 MeV, $\gamma_{\rm s}$=1 [21]. Discrepancies between model and data remain below the systematic uncertainties of the model and among different data sets.

Of course, dynamic systems never freeze out at constant T and μ. While the steep T-dependence of the particle densities (which determine the local scattering rates and control freeze-out [18]) prohibits strong temperature variations across the freeze-out surface [19], incomplete baryon number stopping causes at higher energies significant longitudinal variations of $\mu_{\rm B}$ [16]. A global thermal fit replaces the freeze-out distributions $T_{\rm chem}(x)$, $\mu_{\rm B}(x)$ by average values $\langle T_{\rm chem}\rangle$, $\langle\mu_{\rm B}\rangle$. A recent study by Sollfrank [20], in which he performed a global thermal fit to particle yields from a hydrodynamic calculation, showed that after optimizing $\langle T_{\rm chem}\rangle$ and $\langle\mu_{\rm B}\rangle$ the thermal model predicted yields which differed by up to 15% from the actual ones, although hydrodynamic simulations implement perfect (local) chemical equilibrium by construction. *Thermal model fits can thus never be expected to be perfect*; without detailed dynamical assumptions local variations of the thermal parameters in the real collision can never be fully absorbed by the model. Discrepancies between model and data at the 15-30% level are inside the systematic uncertainty band of the thermal model approach. While being impressed by how thermal models can reproduce the measured particle ratios at this level of accuracy over up to 3 orders of magnitude (see Fig. 3), I am thus deeply suspicious of "perfect" thermal model fits.

A second lesson to be learned from the exercise in [20] is that the χ^2/d.o.f. resulting from such a fit is not very useful as an absolute measure for the quality of the fit: since discrepancies between the real yields and the predictions from the global thermal model cannot be avoided, χ^2/d.o.f. becomes larger and larger as the data become more and more accurate. While χ^2 minimization can still be used to identify the optimal model

parameters within a given model, one should be very careful in using the absolute value of χ^2/d.o.f. to judge the relative quality of different model fits [22].

Let me note that the *ideal system for thermal model fits of particle ratios* will be provided by heavy-ion collisions at RHIC and LHC: hadron formation will happen at the confinement transition, and near midrapidity the baryon density is so low that T_c is nearly independent of μ_B. Replacing $T(x)$ by $\langle T \rangle$ will then be an excellent approximation. Due to longitudinal boost-invariance near midrapidity, knowledge of dN/dy will be good enough for a reliable chemical analysis. Finally, transverse flow can only be stronger at RHIC and LHC than at the SPS, so freeze-out will happen even more quickly after hadronization, strengthening the primordial character of the observed particle ratios.

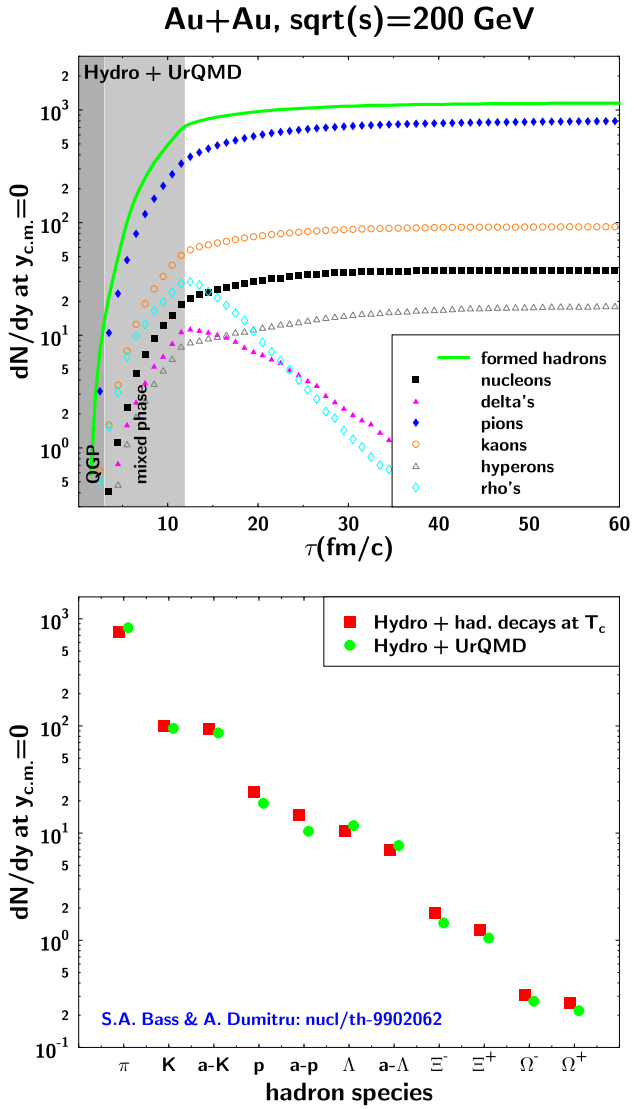

Figure 4.
Upper part: time dependence of midrapidity hadron densities for Au+Au collisions at RHIC, calculated in a combined hydrodynamic + URQMD simulation [13]. At the hadronization temperature T_c hadrons are created from the hydrodynamic phase with chemical equilibrium abundances and are then evolved kinetically by URQMD.
Lower part: final hadron abundances at the end of the kinetic stage (circles) and if the calculation is stopped and all resonances are decayed directly at T_c (squares).

These expectations are borne out by a recent analysis by Bass and Dumitru [13] who combined a hydrodynamic description of the dense early stage with a URQMD simulation of the late hadronic stage. Fig. 4 (bottom) shows that indeed chemical freeze-out occurs quickly after hadronization: the yields at hadronization (squares) and after the last elastic scattering (circles) differ by less than 30%, in spite of many collisions in between [13].

The fit of Pb+Pb data in Fig. 3 [21] yields a chemical freeze-out temperature $T_{\rm chem} \approx$

170 MeV at full strangeness saturation (γ_s=1). In [22] the same data are fit with $T_{\rm chem} = 144 \pm 2$ MeV and a strongly oversaturated strange phase-space ($\gamma_s = 1.48 \pm 0.08$). The authors also allow for oversaturation of the light quarks and find γ_q=1.72±0.08 which allows to absorb the large pion multiplicity at a low value of $T_{\rm chem}$. This "chemical non-equilibrium" [22] fit underpredicts $\bar{\Omega}/\bar{\Xi}$ by 40% and Ω/Ξ by 60%, a problem which disappears at $T_{\rm chem}$=170 MeV (Fig. 3). More importantly, since $\gamma_q^2 = e^{\mu_\pi/T}$, the freeze-out parameters in [22] imply a very large pion chemical potential $\mu_\pi = 156\,{\rm MeV} > m_\pi$; this invalidates the assumption [22] that Bose statistics for pions can be accounted for by considering only the first correction to the Boltzmann term. Hence, while the authors of [22] prefer their fit on the basis of a low χ^2/d.o.f., it has systematic uncertainties which far exceed the statistical errors given in [22].

Having established the location in the phase diagram where chemical freeze-out occurs, we should again ask: *How did the system get there?* Since $T_{\rm chem}$ turns out to be very close to the predicted critical value for the hadronization phase transition, there is clearly no time between hadron formation and chemical freeze-out for kinetic equilibration of the hadron abundances by inelastic hadronic rescattering [3]. The observed hadronic chemical equilibrium at $T_{\rm chem}$ must therefore be *pre-established*: it reflects a statistical occupation of the hadronic phase-space, following the principle of maximum entropy, by the hadronization process [2]. Hadrons form from a prehadronic stage by filling each available phase-space cell with equal probability, subject only to the constraints of energy, baryon number and strangeness conservation (the latter includes a possible overall suppression of strangeness). Afterwards, the chemical composition decouples essentially immediately, without major modifications by hadronic rescattering.

The parameter $T_{\rm chem}$ is thus *not a hadronic temperature in the usual sense*, i.e. not a result of hadronic kinetic equilibration. In the maximum entropy spirit it should be interpreted as a Lagrange multiplier which regulates the hadron abundances in accordance with the conservation laws and is directly related to the critical energy density at which hadronization can proceed. $T_{\rm chem}\approx$170 MeV translates into $\epsilon_c\approx$1 GeV/fm^3. This also explains naturally Becattini's observation [23,2] of hadronic chemical equilibrium at the same value of $T_{\rm chem}$ in e^+e^-, pp and $p\bar{p}$ collisions at essentially all collision energies, although there hadronic final state interactions are completely absent. Whether the constituents of the prehadronic stage themselves thermalize before or during hadronization is a question which final hadron abundances cannot answer; as likely as their thermalization may appear, it is not necessary for an explanation of the observed phenomena.

The concept of statistical hadron formation from a pre-existing state of color-deconfined, completely uncorrelated quarks and antiquarks is supported by a recent analysis[3] of Bialas [25] which follows similar earlier arguments by Rafelski [26] but formulates them more generally such that they do not require thermalization. Bialas points out that by considering baryon/antibaryon (or generally particle/antiparticle) ratios, the unknown effects on hadronization from the internal hadron structure drop out and one can check directly whether the observed hadron abundances can be fully understood by just counting their conserved quantum numbers (carried by their valence quarks), or whether additional correlations among the quarks exist. He finds [25] that in S+S and Pb+Pb collisions at

[3]For an improved argument taking into account global flavor conservation during hadronization see [24].

the SPS the former is true while hadron production yields in p+Pb collisions point to correlations among the quarks.

4. Early memories: strangeness enhancement

The one decisive feature which distinguishes heavy-ion from elementary particle collisions is the strangeness content in the hadronic final state: the global strangeness fraction of the produced quark-antiquark pairs, $\lambda_s = 2\langle s\bar{s}\rangle/\langle u\bar{u}+d\bar{d}\rangle|_{\rm produced}$, is about 2 times higher in nuclear collisions [27,28]. This can not be reproduced by hadronic rescattering models [27,14] and must thus be a feature of the prehadronic state. Here I would like to discuss in more detail the specific enhancement factors for $K, \bar{K}, \Lambda, \bar{\Lambda}, \Xi, \bar{\Xi}, \Omega, \bar{\Omega}$, and ϕ reported recently and during this meeting [29,30].

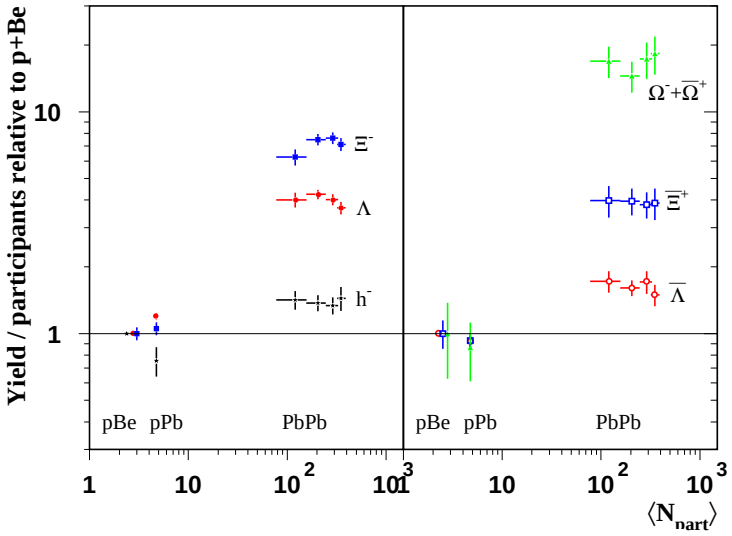

Figure 5. Centrality dependence of strangeness enhancement as measured by WA97 [29,30]. The strange particle yields per participating nucleon in Pb+Pb collisions at the SPS are compared to the same ratio in p+Be and p+Pb collisions.

Fig. 5 shows that the relative strangeness enhancement between Pb+Pb and p+Be collisions is the stronger the more strange quarks the hadron contains. This is perfectly consistent with the above picture of statistical hadronization: disregarding other phase-space constraints, an Ω, for example, which contains 3 strange quarks, is expected to be enhanced by a factor 2^3=8 if strange quarks are enhanced by a factor 2. On the other hand, this pattern contradicts expectations from final state hadronic rescattering: since hadrons with more strange quarks are heavier and strangeness must be created in pairs, the production of stranger particles is suppressed by increasingly higher thresholds.

An interesting observation from Fig. 5 is the apparent centrality independence of the specific strangeness enhancement factors: the enhancement appears to be already fully established in semiperipheral Pb+Pb collisions with about 100 participating nucleons. In fact, the global enhancement by a factor 2 was already seen in S+S collisions by NA35 [27]. Since it must be a prehadronic feature, but the lifetime of the prehadronic stage is shorter for smaller collision systems, this points to a new fast strangeness production mechanism in the prehadronic stage. Exactly this was predicted for the quark-gluon plasma [31].

At this meeting we saw new data on the centrality dependence of hadron yields [30]. Unfortunately, different centrality measures and prescriptions to determine $N_{\rm part}$ have been used. This needs clarification before the pattern in Fig. 5 can be considered confirmed.

Much recent effort went into trying to explain these observations within microscopic

simulations based on string breaking followed by hadronic rescattering. *All such attempts failed.* VENUS and RQMD give more strangeness enhancement for more central collisions [32], however not from hadronic rescattering, but mostly from the non-linear rise of the formation probability for quark matter droplets and color ropes. Strangeness enhancement is thus put in as an initial condition; unlike Fig. 5 it rises monotonically with $N_{\rm part}$. HIJING/$B\bar{B}$ [33] uses baryon junction loops to enhance strange baryon production near midrapidity. Again this puts the enhancement into the initial conditions. The measured $N_{\rm part}$-dependence is not reproduced. The model also disagrees with the observed pattern $\bar{\Omega}/\Omega > \bar{\Xi}/\Xi > \bar{\Lambda}/\Lambda$ (which the statistical hadronization picture [25] explains nicely). Finally, the "improved dual parton model" [34], which gets some fraction of the enhancement in the initial state from "diquark-breaking collisions" and claims to obtain an even larger additional enhancement from hadronic final state interactions, suffers from a severe violation of detailed balance: it only includes inelastic channels (like $\pi+\Xi\to\Omega+K$) which increase multistrange baryons but neglects the (at least equally important [35]) strangeness exchange processes (like $\pi+\Omega\to\bar{K}+\Xi$) which destroy them. Consequently it also fails to reproduce the apparent saturation of the enhancement factors seen in Fig. 5.

The observed strangeness enhancement pattern thus cannot be generated by hadronic final state interactions, but must be put in at the beginning of the hadronic stage. No working model which does so in agreement with the data is known, except for conceptually simplest one, the statistical hadronization model.

5. Summary

The analysis of soft hadron production data at the SPS indicates that hadron formation proceeds by statistical hadronization from a prehadronic state of uncorrelated (color-deconfined) quarks. This leads to pre-established apparent chemical equilibrium among the formed hadrons at the confinement temperature $T_{\rm c}$; it is not caused by kinetic equilibration through hadronic rescattering. After hadronization the hadron abundances freeze out more or less immediately. The chemical freeze-out temperature thus coincides with the critical temperature, $T_{\rm chem} \approx T_{\rm c} \approx$ 170-180 MeV, corresponding to a critical energy density $\epsilon_{\rm c} \approx 1$ GeV/fm^3 as predicted by lattice QCD.

The prehadronic state in $A+A$ ($A\geq$32) collisions contains about twice more strangeness than in e^+e^- and pp collisions. This strangeness enhancement appears to be already fully established in nuclear collisions with 60 or more participant nucleons and can not be generated by hadronic final state interactions. This suggests a fast $s\bar{s}$ creation mechanism in the prehadronic stage, as predicted for a quark-gluon plasma.

A clear hierarchy between chemical ($T_{\rm chem} \approx$ 170–180 MeV) and thermal ($T_{\rm therm} \approx$ 90–100 MeV) freeze-out is observed in Pb+Pb collisions at the SPS; the gap is somewhat smaller ($\approx$ 130–140 MeV vs. $\approx$ 90 MeV) at the AGS. In both cases thermal decoupling is accompanied by strong radial collective flow. The smaller inverse slopes of the Ω $m_\perp$-spectra suggest that a considerable fraction (but probably not all) of this flow is generated by strong elastic hadronic rescattering after hadronization [36].

I conclude that we have seen the Little Bang in the laboratory, and that most likely it is initiated by a quark-gluon plasma.

Acknowledgements: I thank S. Bass, J. Cleymans and R. Lietava for providing me with Figs. 1, 4, and 5. Several fruitful discussions with R. Stock are gratefully acknowledged.

A comment by Zhangbu Xu led to the clarification presented in Footnote 1.

REFERENCES

1. J. Cleymans, K. Redlich, Phys. Rev. Lett. 81 (1998) 5284; and nucl-th/9903063.
2. F. Becattini, U. Heinz, Z. Phys. C76, (1997) 269; U. Heinz, Nucl. Phys. A638 (1998) 357c; J. Phys. G25 (1999) 263; and hep-ph/9902424.
3. R. Stock, Prog. Part. Nucl. Phys. 42 (1999) 295; Phys. Lett. B456 (1999) 277.
4. E. Shuryak, this volume (hep-ph/9906443).
5. E. Schnedermann, U. Heinz, Phys. Rev. C50 (1994) 1675.
6. T. Csörgő, B. Lörstad, Phys. Rev. C54 (1996) 1390; R. Scheibl, U. Heinz, Phys. Rev. C59 (1999) 1585.
7. N. Xu et al. (NA44 Coll.), Nucl. Phys. A610 (1999) 175c.
8. H. Dobler, J. Sollfrank, U. Heinz, Phys. Lett. B457 (1999) 353.
9. U.A. Wiedemann, this volume, and references therein (nucl-th/9907048).
10. H. Appelshäuser et al. (NA49 Coll.), Eur. Phys. J. C2 (1998) 661.
11. See contributions by H. Sorge, M. Bleicher, and W. Cassing in this volume.
12. L. Bravina et al., J. Phys. G25 (1999) 351; hep-ph/9906548; Phys. Lett. B, in press.
13. S. Bass, A. Dumitru et al., nucl-th/9902062.
14. S. Soff et al., nucl-th/9907026.
15. U. Heinz, Nucl. Phys. A566 (1994) 563c; NATO ASI Series B346 (1995) 413.
16. C. Slotta, J. Sollfrank, U. Heinz, AIP Conf. Proc. 340 (1995) 462.
17. J. Sollfrank, U. Heinz, H. Sorge, N. Xu, Phys. Rev. C59 (1999) 1637.
18. J. Bondorf, S.I.A. Garpman, J. Zimányi, Nucl. Phys. A296 (1978) 320.
19. E. Schnedermann, J. Sollfrank, U. Heinz, NATO ASI Series B303 (1993) 175; U. Mayer, U. Heinz, Phys. Rev. C56 (1997) 439.
20. J. Sollfrank, Eur. Phys. J. C9 (1999) 159.
21. P. Braun-Munzinger, I. Heppe, J. Stachel, nucl-th/9903010.
22. J. Rafelski, J. Letessier, nucl-th/9903018.
23. F. Becattini, Z. Phys. C69 (1996) 485.
24. J. Zimányi, T. Biró, P. Lévai, hep-ph/9904501.
25. A. Bialas, Phys. Lett. B442 (1998) 449.
26. J. Rafelski, Phys. Lett. B262 (1991) 333.
27. See discussion by G. Odyniec, Nucl. Phys. A638 (1998) 135c, and references therein.
28. F. Becattini, M. Gaździcki, J. Sollfrank, Eur. Phys. J. C5 (1998) 143.
29. E. Andersen et al. (WA97 Coll.), Phys. Lett. B433 (1998) 209; R. Lietava et al. (WA97 Coll.), J. Phys. G25 (1999) 181 (for the correct Fig. 7 see p. 460 in the same volume); H. Appelshäuser et al. (NA49 Coll.), Phys. Lett. B444 (1998) 523.
30. See F. Antinori, D. Elia (WA97 Coll.); F. Sikler, C. Höhne (NA49 Coll.); and N. Willis (NA50 Coll.), this volume.
31. J. Rafelski, B. Müller, Phys. Rev. Lett. 48 (1982) 1066.
32. F. Antinori et al., Eur. Phys. J. C, in press; R. Caliandro, private communication.
33. S.E. Vance, M. Gyulassy, nucl-th/9901009.
34. A. Capella, C.A. Salgado, hep-ph/9903414.
35. P. Koch, B. Müller, J. Rafelski, Phys. Rep. 142 (1986) 167, Fig. 5.2.
36. H. van Hecke, H. Sorge, N. Xu, Phys. Rev. Lett. 81 (1998) 5764.